

PACS 61.43.Fs, 61.80.Ed, 78.20.-e

## **Metallic nanoparticles (Cu, Ag, Au) in chalcogenide and oxide glassy matrices: comparative assessment in terms of chemical bonding**

**O.I. Shpotyuk<sup>1-3\*</sup>, M.M. Vakiv<sup>1</sup>, M.V. Shpotyuk<sup>5</sup>, S.A. Kozyukhin<sup>4</sup>**

<sup>1</sup>*Institute of Materials of SRC "Carat", 202 Stryjska str., 79031 Lviv, Ukraine*

<sup>2</sup>*O.G. Vlokh Institute of Physical Optics, 23, Dragomanov str., 79005 Lviv, Ukraine*

<sup>3</sup>*Jan Dlugosz University, 13/15 al. Armii Krajowej, Czestochowa, 42200, Poland*

<sup>4</sup>*N.S. Kurnakov Institute of General and Inorganic Chemistry,*

*31, Leninsky Pr., Moscow, 199991, Russia*

<sup>5</sup>*Lviv Polytechnic National University, 12, Bandera str., 79013 Lviv, Ukraine*

\* *The corresponding author e-mail: [olehshpotyuk@yahoo.com](mailto:olehshpotyuk@yahoo.com)*

**Abstract.** Principal difference in origin of high-order optical non-linearities caused by metallic nanoparticles such as Cu, Ag and Au embedded *destructively* in oxide- and chalcogenide-type glassy matrices has been analyzed from the viewpoint of semi-empirical chemical bond approach. The numerical criterion has been introduced to describe this difference in terms of mean molar bond energies character for chemical interaction between unfettered components of destructed *host* glassy matrix and embedded *guest* atoms. It has been shown that "soft" covalent-bonded networks of chalcogenide glasses of As/Ge-S/Se systems differ essentially from glass-forming oxides like silica by impossibility to accommodate agglomerates of metallic nanoparticles. In contrast, such nanostructured entities can be well stabilized in Cu-, Ag- or Au-embedded oxide glasses in full accordance with numerous experimental evidences. Recent unsubstantiated speculations trying to ascribe this ability to fully-saturated covalent matrices of chalcogenide glasses like As<sub>2</sub>S<sub>3</sub> are analyzed and criticized as the misleading and inconclusive ones.

**Keywords:** chalcogenide glasses, glass-forming oxides, surface plasmon resonance, nanoparticle, chemical bond.

Manuscript received 23.11.16; revised version received 20.01.17; accepted for publication 01.03.17; published online 05.04.17.

### **1. Introduction**

In recent years, the glassy-like composites containing embedded metallic nanoparticles (MNPs) occupy an important niche in modern photonics as promising plasmonic media possessing excellent nonlinear optical properties (increased high-order non-linearities) [1-7]. Electro-magnetic excitations of conduction electrons in nanostructured metallic entities, exemplified by agglomerates of externally-embedded silver Ag, gold Au

or copper Cu MNPs, result in *localized surface plasmon resonance* (LSPR), the phenomenon serving as a basis for biomedical sensing with controllable effects on NP size, shape and chemical environment [8]. In this view, *chalcogenide glasses* (ChG), e.g. melt-quenched vitreous compounds of chalcogens (S, Se, Te, but not O) with some elements from IV-V groups of the Periodic Table (Ge, As, Sb, Bi, etc.) [9], which possess few orders higher optical non-linearities as compared with *glass-forming oxides* (GFO) such as fused silica SiO<sub>2</sub> [1, 2,

10], attract high attention. Therefore, from a device standpoint, the chemical-technological approaches allowing further enhancing these non-linearities in different glassy-like matrices seem very important.

Nowadays, different types of technologies have been employed to enhance optical non-linearities in MNPs-embedded glasses, which include thermal-electrical and optical poling, controllable nucleation and crystallization at nano- and microscales, quenching, laser- and/or electron-driven precipitation of metal ions combined with further heat treatment, as well as ion-beam irradiation (ion implantation) [7, 11-15]. Noteworthy, in view of principally different chemistry, not all of these methods are equally suitable for GFO and ChG.

In general, the methods allowing formation of MNPs in a bulk glass can be grouped in *physical*, when these additives are directly introduced in a glassy matrix or previously created MNPs are covered with glassy layer [16-18]), and *chemical*, when MNPs are formed due to *in-situ* chemical interaction of some precursors with a glassy matrix [19]. Physical methods related with direct embedding MNPs, such as ion beam implantation, are known to be *highly destructive* to ensure metastable agglomeration of *guest MNPs* in the *host* glassy matrix, the degree of destruction being strongly dependent on atomic compactness of the latter [7, 20]. In relatively dense GFO containing great amount of silica SiO<sub>2</sub> [6, 7, 15, 20] or network ChG composed by close packing of structural polyhedrons interlinked via chalcogen chains (such as As<sub>2</sub>S<sub>3</sub>, As<sub>2</sub>Se<sub>3</sub>, As/Ge-S/Se, Ge-As/Sb-S/Se) [10, 21], the *host* glassy matrix should be significantly destroyed to accommodate the embedded MNPs. Therefore, the agglomeration occurs under tight chemical interaction between these metallic atoms and components of the destructed glass, the preferential character of this interaction defining geometrical appearance of MNPs (sizes and shapes) and, finally, effect of optical non-linearities.

Thus, the principal difference between GFO and ChG should be carefully examined to clarify expected consequences resulting from embedded MNPs. In this paper, we try to do this from the viewpoint of chemical bond approach [22-24], one of the most productive semi-empirical quantitative route providing valuable insight on atomistic arrangement in solids, put forward by Phillips in the earliest 1970s [25].

## 2. Chemical bonding disproportionality in a glass

Distribution of chemical bonds in a *host* glassy matrix is known to be essentially disturbed under *destructive nanostructurization* such as ion implantation owing to nuclear collisions of implanted ions with target atoms, destruction of bonds and further deionization transforming metallic (M) ions in neutral atoms [20, 26]. Chemical interaction of embedded M atoms (M = Cu, Ag, Au) with unfettered atoms in the glassy-like matrix

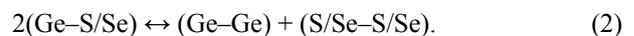
becomes possible under these conditions resulting in new bond distribution.

For As-based ChG like stoichiometric glassy g-As<sub>2</sub>(S/Se)<sub>3</sub>, the bond balance is governed by *thermochemical stability/disproportionality* between *hetero-to-homonuclear bonding* [9]:



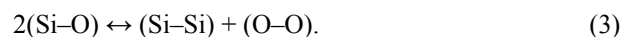
The energetic balance of this reaction (1) is left-shifted attaining 40 kJ/mol for g-As<sub>2</sub>S<sub>3</sub>, as it follows from comparison of mean molar bond energies calculated from standard atomization enthalpies of relevant chemical compounds gathered in Table 1 (such estimation is appreciated within an error-bar of ±10 kJ/mol). Under non-equilibrium conditions (like rapid quenching from high temperatures exceeding the boiling point of As<sub>2</sub>S<sub>3</sub> [9, 27-30]), this reaction can stretch towards right side, thus meaning a great amount of “wrong” homonuclear bonds in the As-S alloy (not typical for stoichiometry of As-S system) and other structural defects, such as charged miscoordinated atoms [9]. With transition to g-As<sub>2</sub>Se<sub>3</sub>, the energetic balance of *hetero-to-homo-nuclear* bonding (1) is only slightly reduced reaching 35 kJ/mol.

The similar consideration can be validated for Ge-based ChG like glassy g-GeS/Se<sub>2</sub>, where *hetero-to-homonuclear bonding disproportionality* can be presented as:



The energetic balance of this reaction (2) is also left-shifted with somewhat higher barrier of 65 kJ/mol for g-GeS<sub>2</sub> and nearly the same 40 kJ/mol for g-GeSe<sub>2</sub>.

The character of chemical bonding disproportionality is not principally changed in GFO, where heteronuclear bonds also prevail over the homonuclear ones. However, energetic balance of corresponding *hetero-to-homonuclear bonding* is strongly enhanced as compared to ChG. Thus, the mean molar energy of Si-O chemical bond in silica (*i.e.* g-SiO<sub>2</sub>) is more than twice favorable than in ChG environment being as high as 465 kJ/mol (see Table 1) [9]. Therefore, the chemical bonding disproportionality in this GFO defined as



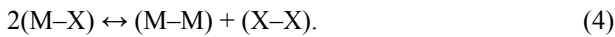
shifts left towards heteronuclear Si-O bonds, subsequently reaching 375 kJ/mol in a balance, that is nearly one order higher as in typical ChG.

This remarkable difference allows wider band-gaps in GFO, making them optically transparent and colorless in the visible spectral range. So, it seems reasonable that this energetically favorable structural arrangement can be notably disturbed only by high-energy destructive influences. That is why dielectric GFO like silica g-SiO<sub>2</sub> are often distinguished as “hard” glasses, in an obvious contrast to semiconductor ChG, which are typically termed as “soft” glasses [31].

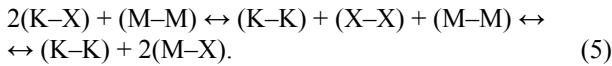
### 3. Generalized energetic $\chi$ -criterion for chemical bonding in destructed glassy matrices

The behavior of small amounts of metallic additives in different ChG environment have been remarkably reviewed in the known monograph by Borisova *et al.* [32] near a three decades ago. In full harmony with this consideration, our preliminary analysis [33, 34] shows that difference in the dissociation energies of chemical bonds composing a *host* glassy matrix for embedded *guest* M ions can be parameterized to serve as a signature for preferential chemical bonding in destructed *host-guest* matrix. Let's generalize this approach to compare the above chemical bonding consideration in respect to reactions (1)-(3) attributed to typical GFO and ChG affected by M ions implantation.

By signing cation-type and anion-type atoms in a glassy target as K and X, respectively (so that K = Si, As, Ge and X = O, S, Se, Te), the chemical disproportionality in such a system under implanted metallic atoms M (M = Cu, Ag, Au) can be presented by analogy with above reactions (1)-(3) via similar *hetero-to-homonuclear bonding disproportionality*



The *generalized disproportionality* under condition of all chemical interactions possible between existing entities (destructed bonds of *host* glassy matrix and implanted *guest* M ions) can be defined as *sequent bond transformation* resulting with respect to reactions (1)-(4) in



Thereby, new balance of *chemical bonding* in a *host* glassy matrix possessing preferential heteronuclear (K-X) environment with embedded destructively M atoms is stabilized in an equilibrium between left and right sides of the above reaction (5). If energetic barrier  $\Delta E$  of his reaction occurs to be positive (right-hand shifted equilibrium), the implanted M atoms destroy existing bond distribution in the host matrix by forming heteronuclear (M-X) bonds at the cost of "wrong" homonuclear (K-K) ones. Otherwise, the agglomeration of MNPs occurs owing to prevalence of (M-M) interaction and renovation of destructed (K-X) bonds.

Thus, we can enter the generalized energetic  $\chi$ -criterion describing agglomeration of MNPs embedded destructively into the host glassy matrix as

$$\chi = 2[M-X] + [K-K] - 2[K-X] - [M-M] = 2([M-X] - [K-X]) + ([K-K] - [M-M]), \quad (6)$$

where notes in square brackets define the mean molar energy of corresponding covalent chemical bonds. The negative values of  $\chi$ -criterion correspond to agglomeration of MNPs in *host* glass, while the positive ones are signatures of preferential interaction between M atoms and unfettered atoms of destructed glass (K and X) resulting in a mixed metal-glass matrix.

The mean molar energies of heteronuclear (M-X) bonds for M atoms (M = Cu, Ag, Au) in GFO and ChG environment calculated as bond dissociation energies in diatomic molecules [35] are given in the comparative diagram in Fig. 1. Under a comparison with Table 1, it is evident these bond energies are essentially reduced as those character for Si-O bonds in g-SiO<sub>2</sub>, while they are comparable and even slightly greater than dissociation energies of heteronuclear bonds in ChG. It means that under ion implantation the destructed Si-O bonds in g-SiO<sub>2</sub> will be renewed, facilitating agglomeration of "pure" MNPs in a host bulk (provided implantation dose is sufficient to ensure rather high MNPs excess above the solubility limit [7, 20, 26]). It is worth to note that, in respect to the calculated  $\chi$ -criterion, agglomeration of Au MNPs in oxide environment has an obvious preference ( $\chi = -480$  kJ/mol) over other metallic additives.

Hence, the  $\chi$ -criterion for chemical bonding (6) is strongly negative for GFO like silica glass g-SiO<sub>2</sub> (Fig. 1). However, this is not a case of ChG, where  $\chi$ -criterion is nearly one-order smaller as in GFO. This is clearly revealed for Cu atoms embedded destructively in environment of As-S, As-Se, Ge-S or Ge-Se chemical bonds. For Ag and Au atoms in sulphide As-S or Ge-S bond environment, the  $\chi$ -criterion becomes negative, but still does not exceeding a few tens of kJ/mol. Thus, it means that in all these cases the clustering of MNPs is principally impossible.

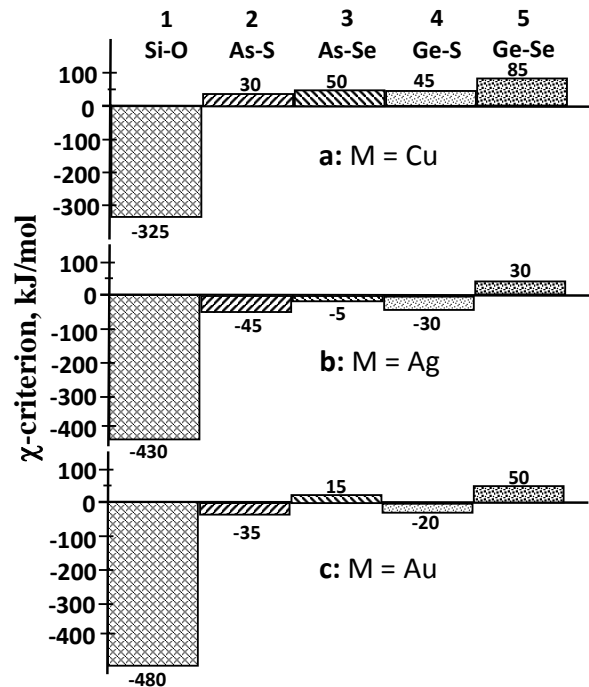


Fig. 1. Comparative diagram of  $\chi$ -criterion (kJ/mol) values for Cu (a), Ag (b) and Au (c) atoms embedded in Si-O (1), As-S (2), As-Se (3), Ge-S (4) and Ge-Se (5) chemical bond environment.

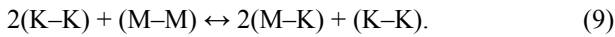
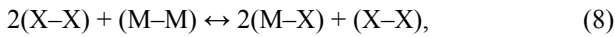
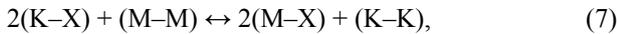
**Table 1. Mean molar bond energies  $E$  for main glass-forming cations in oxide and chalcogenide environment [9].**

Bond	$E$ , kJ/mol						
As-As	200	Ge-Ge	185	Si-Si	225	O-O	330*
As-O	335	Ge-O	355	Si-O	465	S-S	280
As-S	260	Ge-S	265	Si-S	310*	Se-Se	225
As-Se	230	Ge-Se	225	Si-Se	270*	Te-Te	195
As-Te	205	Ge-Te	200	Si-Te	230		

Note: \* - corrected under bond dissociation energies for diatomic molecules taken from [35].

#### 4. Non-stoichiometry effects in M-embedded ChG matrices

Noteworthy, the ChG (contrary to GFO) can be subjected to stretched variation in their chemistry allowing non-stoichiometric chalcogen and cation-rich glass-forming alloys [9]. But this specificity does not change essentially the above energetic consideration [36]. Indeed, with account of non-stoichiometry, the *generalized disproportionality* reaction (5) can be considered separately for intermetallic (M-M) bonding in heteronuclear (K-X) and homonuclear (K-K) and (X-X) environments, the corresponding reactions being as follows:



The energetic preference of resulting bond balance in a glass can be estimated by accepting weighting coefficients  $\eta$  of different bonds possible under a given structural model:

$$\begin{aligned} &\eta_{K-X}[2(K-X) + (M-M)] + \eta_{X-X}[2(X-X) + (M-M)] + \eta_{K-K}[2(K-K) + (M-M)] \leftrightarrow \\ &\leftrightarrow \eta_{K-X}[2(M-X) + (K-K)] + \eta_{X-X}[2(M-X) + (X-X)] + \eta_{K-K}[2(M-K) + (K-K)]. \end{aligned} \quad (10)$$

where left side reflects energetic balance of agglomerated MNP within renewed *host* matrix, and right side corresponds to M atoms interacting with unfettered atoms of destructed glass.

In real non-stoichiometric ChG media, chemical interaction between embedded M and cation-type K atoms can be ignored in view of smaller bond energies [9], thus resulting in importance of only two first components in both left and right sides of the above reaction (10) to calculate the energetic  $\chi$ -criterion in non-stoichiometric ChG matrices:

$$\begin{aligned} \chi^{st} = &\eta_{K-X}[2(M-X) + (K-K)] + \eta_{X-X}[2(M-X) + (X-X)] - \\ &- \eta_{K-X}[2(K-X) + (M-M)] - \eta_{X-X}[2(X-X) + (M-M)] = \\ = &\eta_{K-X}[2(M-X) - 2(K-X) + (K-K) - (M-M)] + \eta_{X-X}[2(M-X) - (X-X) - (M-M)]. \end{aligned} \quad (11)$$

**Table 2. Mean molar bond energies  $E$  (kJ/mol) of metallic atoms (M = Cu, Ag, Au) in GFO and ChG environment [35].**

Bond	$E$ , kJ/mol	Bond	$E$ , kJ/mol	Bond	$E$ , kJ/mol
Cu-Cu	200	Ag-Ag	165	Au-Au	225
Cu-O	290	Ag-O	220	Au-O	225
Cu-S	275	Ag-S	220	Au-S	255
Cu-Se	255	Ag-Se	210	Au-Se	250

Accepting the values of molar bond energies summarized in Tables 1 and 2 for ChG within the chemically ordered covalent network model (COCNM) [9], it can be easily shown that over-stoichiometric chalcogen atoms only enhances  $\chi$ -criterion, facilitating incorporation of M atoms into the glass matrix, while over-stoichiometric As or Ge has no essential effect on chemical bonds.

So, destructed bonds in host ChG matrix do not recover after destruction, being replaced by more energetically favorable (M-X) bonds. This process results in extraction of metal chalcogenide phase instead of “pure” MNPs. Excess K atoms appearing under this destruction migrate towards surface for further interaction with environment. Undoubtedly, just this impurity interaction is responsible for  $As_2O_3$  extraction at the surface of g- $As_2S_3$  under prolonged  $\gamma$ -irradiation in ambient conditions [36, 37]. Similar changes occur also in Ge-based ChG affected by *cw* laser illumination [38].

#### 5. Experimental evidences on MNPs formation in glassy substances

The above consideration with energetic  $\chi$ -criterion for *MNPs clustering* in a glass (6) concerns *destructed host glassy matrices*, when chemical interaction between some unfettered atoms of glassy target and embedded M atoms cannot be neglected. As it occurs in GFO (or other alternative media with high negative  $\chi$ -criteria like those given in diagram in Fig. 1 for M=Cu, Ag, Au in Si-O bonding environment), ion implantation or other

destructive technology results in agglomeration of MNPs, this process being defined by *destruction efficiency* of *host* matrix (like dose and energy of implanted ions). Typical variants of practical realization of these nanostructurization technologies can be well exemplified by research of Stepanov with co-authors [7, 20, 26] showing enhancement of optical non-linearities in oxide dielectric media due to ion-synthesized MNPs.

However, this is not a case of *nanostructurization* under *non-disturbed* (or partially disturbed) *bond balance* in a *host* glassy matrix, which possibly occurs under positive values of  $\chi$ -criterion presented in Fig. 1 for M atoms in ChG-type bonding. The latter can be illustrated by ChG deposition on MNPs initially formed at a surface of dielectric substrate, when upper glassy film play the role of a covering layer ensuring necessary difference in the refractive index  $n$  with MNPs [16-18]. Because of lack of essential disturbances in chemical interaction within MNPs themselves and neighboring medium, Kokenyesi with co-authors [16-18] observe, in fact, the islands of embedded MNPs in homogeneous ChG environment.

Chemical interactions are also partially suppressed under condition of photostimulated diffusion of M atoms (mainly Ag and Cu) into ChG films [39-41], the famous research launched by Kostishin with co-authors [39] nearly a half century ago. Light illumination causes local misbalance of negative-positive electrical charge in the film due to excitation of chalcogen *lone-pair* electrons, resulting in transfer of electrically neutral M atom into positively-charged  $M^+$  ions [40]. These  $M^+$  ions diffuse along sites of chalcogen atoms, thus leaving principal glass-forming structural units without essential changes, as it was convincingly proved by Stronski with co-authors [41] for Ag-photodoped  $As_2S_3$  films. The M additives stretch in a *host* amorphous matrix, being involved preferentially in coordinative bonding with chalcogen atoms along their diffusion paths, whereas normal covalent bonding occurs only near structural defects [41]. Doubtless, if point getters for *guest*  $M^+$  ions were stabilized in *host* ChG film, it could be possible to create photoexposure-guided agglomerates of MNPs.

Other example concerns the case, when chemical *host-guest* interaction can be ignored due to looser (inhomogeneous) structures of some glassy-like targets. Such research can be well exemplified by experiments on Ag-ions implantation in *chalcocalide matrices* performed by Liu et al. [42, 43]. It was found that in  $56GeS_2-24Ga_2S_3-20KBr$  glass Ag ions embedded under implantation with varied doses from  $10^{16}$  to  $2 \cdot 10^{17}$  ions/cm<sup>2</sup> can be agglomerated presumably in inner spaces of lower densities, which allow appearance of relatively large MNPs agglomerates reaching in sizes even a few hundred nanometers. The enhanced third-order optical non-linearities in these nanostructurized chalcocalide glasses were shown to correlate strongly with ion implantation doses and geometrical sizes of agglomerated Ag MNPs [42, 43]. Recently [44], it was shown that similar results could be achieved under Ag

ions implantation in melt-quenched  $72GeS_2-18Ga_2S_3-10CdS$  glass, the typical sizes of Ag MNPs being ranged from  $\sim 90$  nm (at  $10^{16}$  ions/cm<sup>2</sup> dose) to 300 nm (at  $2 \cdot 10^{17}$  ions/cm<sup>2</sup> dose). This glassy target does not belong to typical structurally-homogeneous ChG like  $g-As_2(S/Se)_3$  possessing glass-forming network with fully saturated and uniform covalent bonding (for more details, see [9, 45] and literature therein). Appearance of large agglomerates of Ag MNPs in this case follows from principal difference in chemical interaction between embedded Ag ions and structurally-specific glass components.

In an obvious contrast to the above argumentation, we should also consider here the example on MNPs clustering in ChG media *in a denial sense* as a result of misleading speculations of some authors [46-48] trying to ascribe unique clustering ability to M atoms embedded destructively in all glassy substances (both GFO and ChG) despite their chemical nature. Thus, Kavetsky with co-authors [46] claimed recently a principal possibility to form agglomerates of ion-implanted Cu MNPs in  $g-As_2S_3$  and  $g-Ge_{15.8}As_{21}S_{63.2}$  like it occurred in silica glass  $g-SiO_2$  [15]. They asserted that Cu MNPs could be gathered in spherical entities of only 5 to 10 nm in radius, giving essential changes in optical linear absorption at  $\sim 580 \dots 590$  nm and response in nonlinear optical properties observed in Z-scan measurements. However, even preliminary and very unscrupulous insight gives an uncontroversial prove on speculative character of such "conclusions".

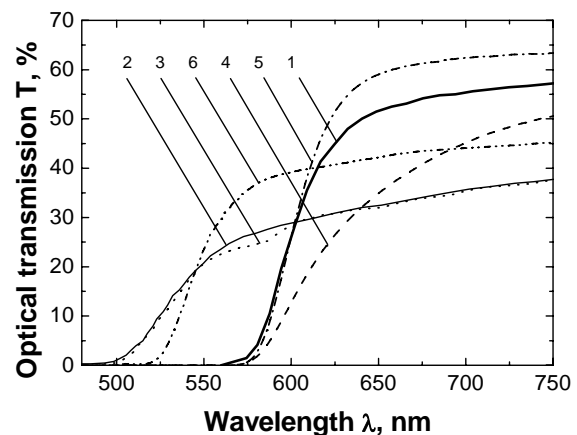


**Fig. 2.** Comparison of optical transmission spectra of As-S ChG (all the samples are  $\sim 1.0$  mm in thickness):  $g-As_2S_3$  before  $\gamma$ -irradiation (1) as compared with that of Fig. 14.1 from Ref. [48],  $g-As_2S_3$  before (2) and after  $Cu^+$  ion implantation with  $1.5 \cdot 10^{17}$  cm<sup>-2</sup> dose (3) as compared with that of Fig. 14.7 from Ref. [48];  $g-As_2S_3$  prepared, respectively, by quenching from high-temperature 900 °C (4) or low-temperature 500 °C state (5) as compared with that of Ref. [30]; S-rich  $g-As_{22}S_{78}$  affected by phase separation caused by long-term aging (6) as compared with that of Ref. [52]. The spectral positions of optical transmission edges were reproduced without measuring points directly from indicated sources.

First, the characteristic band of LSPR for Cu MNPs in g-As<sub>2</sub>S<sub>3</sub> with the refraction index  $n \cong 2.5$  was attributed to ~580...590 nm domain, which is the characteristic frequency of LSPR in oxide environment with much smaller  $n$  (below 2.0) [7]. In concomitance with oxide matrices (such as SiO<sub>2</sub>, Al<sub>2</sub>O<sub>3</sub>, ZnO, etc.) [7, 15, 26], this LSPR band positioned in accordance to known formula for spherical MNPs [49] should be expected in ChG with refraction indices  $n > 2.4$  only at longer wavelengths (more than 620...630 nm), but not at the shorter ones (~580...590 nm).

Second, the results of Z-scan patterning (which was presented as a main evidence for enhanced optical nonlinearities in [46-48]) were given only for Cu-implanted ChG affected by laser irradiation at various intensities, but not compared with parent non-implanted specimen. So, it was impossible at all to conclude (even intuitively) on probable origin of this "effect". As an example of rational and unbiased consideration on this issue, we refer to known works of Almeida *et al.* [50, 51] on open aperture Z-scan signatures of nonlinear optical absorption caused by Au MNPs in heavy-metal oxide glasses of GB type (*i.e.* GeO<sub>2</sub>-Bi<sub>2</sub>O<sub>3</sub>). All these evidences were always grounded on reliable comparison between non-affected (parent) GB glasses and these glasses affected by embedded Au MNPs (GB-Au). Such experimental purity including obligatory comparison with reference specimen (non-affected or parent) was also a necessary condition for conclusion on third-order optical non-linearity from ion-implanted Ag MNPs in the cited Liu's research [42-44].

Third, it seems doubtful (if any) to adopt unambiguously that optical transmission spectrum in [46-48] can be really ascribed to stoichiometric g-As<sub>2</sub>S<sub>3</sub> of ~1 mm in thickness. For more convincing argumentation on this issue, different optical transmission spectra for As-S ChG taken additionally from [30, 52] are compared as depicted in Fig. 2. As a top of full misunderstanding, it should be emphasized huge difference of more than 50 nm (!) in the wavelength position of optical transmission edge for the same g-As<sub>2</sub>S<sub>3</sub> measured before ion implantation and gamma-irradiation in Ref. [48]. Comparison with ChG prepared in different quenching regimes [30] testifies that latter is rather appropriate for g-As<sub>2</sub>S<sub>3</sub>, but not spectra depicting short-wave optical transmittance (500...550 nm) in Ref. [46-48]. Within careful inspection of As-S system [52], it seems that only non-stoichiometric S-rich ChG transmit incident light near ~500 nm, but at obviously higher transparency (as compared with that of the Fresnel formula [53]), the 69% in optical transmission corresponds to refractive index  $n \cong 2.5$ . So, their allegation on ion implantation in g-As<sub>2</sub>S<sub>3</sub> [46-48] is roughly falsified and simply speculative.

It was also strange why implantation in [46-48] arranged at higher doses (10<sup>17</sup> ion/cm<sup>2</sup>) did not change optical transmission of implanted ChG giving *point-to-point* coincidence with data for initial non-implanted ChG in the whole spectral range excepting the 580...590 nm

part (see Fig. 2). So, it seems that the authors of [46-48] deal with inhomogeneous ChG (probably, one of S-enriched compositions close to g-As<sub>2</sub>S<sub>8</sub>, provided ChG of As-S system was really used), which have been destructed just preliminary, *i.e.* before implantation (maybe due to poor mechanical treatment or invalid quenching route applied to stabilize ChG), and thus their claim on full identity between ion implantation in GFO and ChG is entirely misleading and inconclusive.

## 6. Conclusions

In summary, we would like to underline the principal difference in the origin of high-order optical nonlinearities related with metallic nanoparticles embedded destructively in oxide- and chalcogenide glassy matrices. The chemical bonding approach is adequately applied to describe this difference in terms of the mean molar bond energies typical for interaction between unfettered atoms of host glassy network and embedded guest atoms (Cu, Ag, Au). Corresponding energetic barriers of bond disproportionality for metallic atoms defined as  $\chi$ -criterion occur to be principally different in oxide and chalcogenide environment. These findings are in full agreement with numerous experiments exploring destructive and non-destructive mechanisms of embedding the metallic nanoparticles, but contradict principally to misleading speculations with unproved schemes for nanostructurization in ion-implanted chalcogenide glass networks.

## Acknowledgement

The authors acknowledge support from Science and Technology Center in Ukraine under Pr. No 6174. Discussions on surface plasmon resonance in noble-metal media with N. Dmitruk and I. Blonsky, as well as helpful comments on optical nonlinearities in glasses from V. Kadan are kindly acknowledged.

## References

1. Zakery A., Elliott S.R. *Optical Non-linearities in Chalcogenide Glasses and their Applications*. Berlin-Heidelberg, Springer-Verlag, 2007.
2. Zakery A., Shafmirzaee H. Modeling of enhancement of nonlinearity in oxide and chalcogenide glasses by introduction of nanometals. *Phys. Lett. A*. 2007. **36**. P. 484-487.
3. Tanaka K. Optical nonlinearity in photonic glasses. *J. Mater. Sci.: Mater. Electron.* 2005. **16**. P. 633-643.
4. Tao H., Zhao X., Liu Q. Optical non-linearity in nano- and micro-crystallized glasses. *J. Non-Cryst. Solids*. 2013. **377**. P. 146-150.
5. Ogusu K., Shinkawa K. Optical nonlinearities in As<sub>2</sub>Se<sub>3</sub> chalcogenide glasses with Cu and Ag for pulse durations on the order of nanoseconds. *Opt. Exp.* 2009. **17**. P. 8165-8172.

6. Ganeev R.A., Ryasnyansky A.I. Nonlinear optical characteristics of nanoparticles in suspensions and solid matrices. *Appl. Phys. B*. 2006. **84**. P. 295–302.
7. Stepanov A.L. Nonlinear optical properties of implanted metal nanoparticles in various transparent matrixes: A review. *Rev. Adv. Mater. Sci.* 2011. **27**. P. 115–145.
8. Anker J.N., Hall W.P., Lyandres O., Chan N.C., Zhao J., Van Duyne R.P. Biosensing with plasmonic nanosensors. *Nature Materials*. 2006. **7**. P. 442–453.
9. Feltz A. *Amorphous Inorganic Materials and Glasses*. VCH Publ., New York, 1993.
10. Liu Q., Zhao X. Non-linear optical properties of chalcogenide and chalcohalide glasses. *J. Non-Cryst. Solids*. 2010. **356**. P. 2375–2377.
11. Grabiec M., Wolak A., Veron O., Blondeau J.-P., Pellerin N., Allix M., Pellerin S., Dzierzega K. Laser-driven precipitation of silver nanoparticles in soda lime glass matrix monitored by on-line extinction measurements. *Plasmonics*. 2012. **7**. P. 279–286.
12. Podsvirov O.A., Sidorov A.I., Tsekhomskii V.A., Vostokov A.V. Formation of copper nanocrystals in photochromic glasses under electron irradiation and heat treatment. *Phys. Solid State*. 2010. **52**. P. 1906–1909.
13. Rycenga M., Cogley C.M., Zeng J., Li W., Moran C.H., Zhang Q., Qin D., Xia Y. Controlling the synthesis and assembly of silver nanostructures for plasmonic applications. *Chem. Rev.* 2011. **111**. P. 3669–3712.
14. Zeng H., Zhao C., Qiu J., Yang Y., Chen G. Preparation and optical properties of silver nanoparticles induced by a femtosecond laser irradiation. *J. Non-Cryst. Solids*. 2007. **300**. P. 519–522.
15. Ganeev R.A., Ryasnyansky A.I., Stepanov A.L., Usmanov T. Saturated absorption and reverse saturated absorption of Cu:SiO<sub>2</sub> at  $\lambda = 532$  nm. *phys. status solidi (b)*. 2004. **241**. P. R1–R4.
16. Charnovych S., Kokenyesi S., Glodán Gy., Csik A. Enhancement of photoinduced transformations in amorphous chalcogenide film via surface plasmon resonances. *Thin Solid Films*. 2011. **519**. P. 4309–4312.
17. Charnovych S., Dmitruk N., Voynarovych I., Yurkovich N., Kokenyesi S. Plasmon-assisted transformations in metal-amorphous chalcogenide light-sensitive nanostructures. *Plasmonics*. 2012. **7**. P. 341–345.
18. Charnovych S., Dmitruk N., Yurkovich N., Shpiyak M., Kokenyesi S. Photo-induced changes in a-As<sub>2</sub>S<sub>3</sub>/gold nanoparticle composite layer structures. *Thin Solid Films*. 2013. **548**. P. 419–424.
19. Burunkova J., Csarnovics I., Denisyuk I., Daroczi L., Kokenyesi S. Enhancement of laser recording in gold/amorphous chalcogenide and gold/acrylate nanocomposite layers. *J. Non-Cryst. Solids*. 2014. **402**. P. 200–203.
20. Stepanov A.L. Peculiarities of synthesis of metal nanoparticles in dielectrics by ion implantation method. *Vestnik Nizhegorod. Univ.: Ser. Fizika Tverd. Tela*. 2003. **1**. P. 82–88 (in Russian).
21. Nasu H., Kubodera K., Kobayashi M., Nakamura M., Kamiya K. Third-harmonic generation from some chalcogenide glasses. *J. Amer. Ceram. Soc.* 1990. **73**, P. 1794–1796.
22. Bicerano J., Ovshinsky S.R. Chemical bond approach to the structures of chalcogenide glasses with reversible switching properties. *J. Non-Cryst. Solids*. 1985. **74**. P. 75–84.
23. Tichy L., Ticha H. Covalent bond approach to the glass-transition temperature of chalcogenide glasses. *J. Non-Cryst. Solids*. 1995. **189**. P. 141–146.
24. Kastner M. Compositional trends in the optical properties of amorphous lone-pair semiconductors. *Phys. Rev. B*. 1973. **7**. P. 5237–5252.
25. Phillips J.C. Ionicity of the chemical bond in crystals. *Rev. Mod. Phys.* 1970. **42**. P. 317–356.
26. Stepanov A.L., Khaibullin I.B. Fabrication of metal nanoparticles in sapphire by low-energy ion implantation. *Rev. Adv. Mater. Sci.* 2005. **9**. P. 109–129.
27. Yang C.Y., Sayers D.E., Paesler M.A. X-ray-absorption spectroscopy studies of glassy As<sub>2</sub>S<sub>3</sub>. The role of rapid quenching. *Phys. Rev. B*. 1987. **36**. P. 8122–8128.
28. Kuznetsov S.L., Mikhailov M.D., Pecheritsyn I.M., Turkina E.Yu. Structural chemical processes at the synthesis of chalcogenide glasses. *J. Non-Cryst. Solids*. 1997. **213-214**. P. 68–71.
29. Mamedov S., Kisliuk A., Quitmann D. Effect of preparation conditions on the low frequency Raman spectrum of glassy As<sub>2</sub>S<sub>3</sub>. *J. Mater. Sci.* 1998. **33**. P. 41–43.
30. Shpotyuk O., Kozyukhin S., Shpotyuk Ya., Demchenko P., Mitsa V., Veres M. Coordination disordering in near-stoichiometric arsenic sulfide glass. *J. Non-Cryst. Solids*. 2014. **402**. P. 236–243.
31. Musgraves J.D., Richardson K., Jain H. Laser-induced structural modification, its mechanisms, and applications in glassy optical materials. *Opt. Meter. Exp.* 2011. **1**. P. 921–935.
32. Borisova Z.U., Bychkov E.A., Tverianovich Yu.S. *Interaction of Metals with Chalcogenide Glasses*. Leningrad State University Publ., 1991 (in Russian).
33. Shpotyuk O., Shpotyuk M., Cebulski J. On the energetic criterion for destructive clustering of metallic nanoparticles in chalcogenide and oxide glassy matrices. *phys. status solidi (b)*. 2016. **253**. P. 494–498.
34. Shpotyuk M.V., Shpotyuk O.I., Cebulski J., Kozyukhin S. Destructive clustering of metal nanoparticles in chalcogenide and oxide glassy matrices. *Nanoscale Res. Lett.* 2016. **11**. P. 34-1–34-6.

35. Luo Y.-R. *Comprehensive Handbook of Chemical Bond Energies*. Taylor & Francis Group, CRC Press: Boca Raton, 2007.
36. Shpotyuk M., Shpotyuk O., Golovchak R., Demchenko P. FSDP-related correlations in  $\gamma$ -irradiated chalcogenide semiconductor glasses: The case of glassy arsenic trisulphide g-As<sub>2</sub>S<sub>3</sub> revised. *J. Phys. Chem. Solids*. 2013. **74**. P. 1721–1725.
37. Shpotyuk M., Shpotyuk O., Serkiz R., Demchenko P., Kozyukhin S. Surface oxidation in glassy arsenic trisulphide induced by high-energy  $\gamma$ -irradiation. *Rad. Phys. Chem*. 2014. **97**. P. 341–345.
38. Lovas G., Mitsa V., Holomb R., Rosola I., Borkach E. The room temperature visible photoluminescence in g-As<sub>2</sub>S<sub>3</sub> and Ge-based glasses. *Sci. Bull. Uzhgorod Univ. Ser. Fiz*. 2013. **34**. P. 54–58.
39. Kostishin M.T., Michailovskaya E.V., Romanenko P.F. On the effect of photographic sensitivity of thin semiconductor layers on the metal substrate. *Sov. Phys. Solid State*. 1966. **8**. P. 571–576.
40. Elliott S.R. Photodissolution of metals in chalcogenide glasses: a unified mechanism. *J. Non-Cryst. Solids*. 1991. **137–138**. P. 1031–1034.
41. Stronski A.V., Vlcek M., Stetsun A.I., Sklenar A., Shepeliavyj P.E. Raman spectra of Ag- and Cu-photodoped chalcogenide films. *Semiconductor Physics, Quantum Electronics and Optoelectronics*. 1990. **2**. P. 63–68.
42. Liu Q., He X., Zhao X., Ren F., Xiao X., Jiang C., Zhou H., Zhao X., Lu L., Qian S. Third-order nonlinearity in Ag-nanoparticles embedded 56GeS<sub>2</sub>-24Ga<sub>2</sub>S<sub>3</sub>-20KBr chalcogenide glass. *J. Non-Cryst. Solids*. 2011. **357**. P. 2320–2323.
43. Liu Q., He X., Zhao X., Ren F., Xiao X., Jiang C., Zhou X., Lu L., Zhou H., Qian S., Poumellec B., Lancry M. Enhancement of third-order nonlinearity in Ag-nanoparticles-contained chalcogenide glass. *J. Nanopart. Res*. 2011. **13**. P. 3693–3697.
44. Song M., Liu Q.M., Xu Gai G., Ren F. Enhancement of third-order optical nonlinearities in 72GeS<sub>2</sub>-18Ga<sub>2</sub>S<sub>3</sub>-10CdS glasses by ion implantation. *Chalcogenide Lett*. 2015. **12**. P. 453–460.
45. Shpotyuk O., Golovchak R., Kozdras A. Physical ageing of chalcogenide glasses, in: *Chalcogenide Glasses: Preparation, Properties and Applications*, Eds. J.-L. Adam, X. Zhang. Woodhead Publishing series in electronic and optical materials. Oxford: Woodhead Publishing, 2014. P. 209–264.
46. Kavetsky T.S., Valeev V.F., Nuzhdin V.I., Tsmots V.M., Stepanov A.L. Optical properties of chalcogenide glasses with ion-synthesized copper nanoparticles. *Techn. Phys. Lett*. 2013. **39**. P. 1–4.
47. Kavetsky T., Stepanov A.L., Bazarov V.V., Tsmots V., Ren J., Chen G., Zhao X. Comparative study of optical properties of polarizing oxide glasses with silver nanorods and chalcogenide glasses with copper nanoparticles. *Phys. Procedia*. 2013. **48**. P. 191–195.
48. Kavetsky T.S., Stepanov A.L. Effects of gamma-irradiation and ion implantation in chalcogenide glasses. Chapter 14, in: *Glass Nanocomposites: Synthesis, Properties and Applications*. Eds. B. Karmakar, K. Rademann, A.L. Stepanov. Elsevier Acad. Press, 2016. P. 341–358.
49. Blonsky I.V. Femtooptics of films and nanoparticles of noble metals. *Ukr. J. Phys. Repts*. 2009. **5**. P. 170–202.
50. Almeida J.M.P., da Silva D.S., Kassab L.R.P., Zilio S.C., Mendonça C.R., De Boni L. Ultrafast third-order optical nonlinearities of heavy metal oxide glasses containing gold nanoparticles. *Opt. Mater*. 2014. **36**. P. 829–832.
51. Almeida J.M.P., Almeida G.F.B., Boni L., Mendonça C.R. Nonlinear optical properties and femtosecond laser micromachining of special glasses. *J. Braz. Chem. Soc*. 2015. **26**. P. 2418–2429.
52. Golovchak R., Shpotyuk O., McCloy J.S., Riley B.J., Windisch C.F., Sundaram S.K., Kovalskiy A., Jain H. Structural model of homogeneous As-S glasses derived from Raman spectroscopy and high-resolution XPS. *Phil. Mag*. 2010. **90**. P. 4489–4501.
53. Born M., Wolf E. *Principles of Optics*. Cambridge Univ. Press, Cambridge, 1999.